



# Conceptual Analysis and Design and Experimental Construction of a Portable Emergency Relief Bridge

Ehsan Soltani <sup>a,\*</sup>, Shahrokh Rezaei<sup>b</sup>

<sup>a</sup>Department of Civil Engineering, Roudehen Branch, Islamic Azad University, Roudehen, Iran

<sup>b</sup> Department of Civil Engineering, Faculty of Engineering and Flight Imam Ali University, Tehran, Iran

Received 23 November 2021, Accepted 4 October 2022

## Abstract

For a long time, our country has faced natural disasters. In recent years, it has imposed various levels of damages on the country, including those caused by wars (military maneuvers) and natural disasters (earthquakes such as Rudbar Manjil, Bam, and Azgeleh), and floods in cities and regions). Every year, severe floods, hurricanes, explosions, and terrorist attacks cause great suffering for millions worldwide. In a disaster, whether natural or humanitarian, it is vital to provide immediate help to those affected, but relief can often be severely interrupted, significantly if the infrastructure is damaged and the transport network is disrupted. Here, the bridge will be constructed from nonidentical prefabricated elements based on modularity. Construction of modules and final assembly is done off-site (in a factory). Because it can be deployed on-site, it transported the completed bridge in a compact form. SAP2000 software evaluated an emergency bridge's seismic design and performance using nonlinear static and dynamic analysis to save lives in the shortest amount of time, cost, construction, and installation, while also considering the structure's performance. Also, its portability is the goal of this structure. In this system, space structures were used to design the project, absorbing much energy outside their elastic range and was innovative. As a result, the ultimate bearing capacity of the space trusses will depend on the structure's geometry, the position of the supports, and the displacement load response of each member.

**Keywords:** Emergency Relief Bridge, Seismic Performance, Nonlinear Static and Dynamic Analysis, Space Structure.

## 1-Introduction

It is essential to communicate between the two points in the shortest possible time and during the golden age of first aid, which has been cut off due to natural disasters. The impossibility of timely transportation of food, water, medicine, or transfer of the injured to medical centers leads to increased casualties and secondary damages. Therefore, in this study, preliminary studies on the history of first-aid bridges, load analysis, and design of phase zero of this type of bridge are done based on the rapid construction of these bridges. In the aftermath of a natural disaster, all efforts are dedicated to a common goal: repairing and bringing the affected communities back to their fully functioning condition. However, it is frequently encountered that infrastructure and roads providing access to these communities are also damaged, complicating the

restoration activities. Therefore, deployable infrastructure, which can provide means of communication to the affected areas rapidly, is vital for an efficient post-disaster relief effort. Immediate relief, including the distribution of supplies and the restoration of power, was delayed due to the inaccessibility to the affected locations. Similarly, other natural disasters such as landslides, earthquakes, flooding, and tsunamis have caused significant damage to infrastructure. For example, several bridges were destroyed and swept away in Indonesia by the 2004 Great Sumatra Earthquake and Indian Ocean Tsunami, leaving many small communities isolated [1]. Deployable temporary bridges were installed to maintain lines of communication, while new permanent bridges were being designed under new earthquake codes [2]. The

 \*Corresponding Author: Email Address:ehsan.soltany\_te@yahoo.com

large degree of devastation caused by various natural disaster events, how disaster relief is a common need throughout the world, and how deployable structures can potentially be used. Furthermore, although the need for post-disaster relief may increase due to the expected increase in natural and manufactured disasters [3], there is very little research on modifying or improving the existing temporary bridge designs. At the moment, the majority of these were designed in the mid-20th century by the military for military loading requirements [3-4]. Although reliable, when used for civilian applications, these bridges are subjected to smaller load conditions and therefore are conservative. Developing a bridge design that would serve the load conditions specifically required for civilian applications can potentially provide an alternative system that is lighter and more efficient. While the primary motivation for this research is the use of deployable structures for immediate relief, there exists the potential of using the design process and concept for other applications. Examples of these are scaffolding, temporary infrastructure for construction access, and temporary supports for new infrastructure. A deployable structure can volumetrically transform from a compact state to a more significant deployed state when energy is applied to it [5]. Deployable structures are versatile systems with uses in diverse fields, often for their storage and transportation benefits. A familiar example of a deployable system is the umbrella. Umbrellas can be folded when not in use and transformed to a more extensive system after a force is applied.

On a larger scale, deployable structures are used on applications ranging from temporary architectural and civil structures to space applications [6,7]. These include deployable shelters, roofs for stadiums, interim stages, scissor lifts, temporary bridges, solar space arrays, and deployable space antennas [5,6,8,9]. The structures need to meet two different equilibrium requirements: one when they are folded and one when they are expanded static load-bearing systems during operations. Moreover, a deployable structure must also perform as a reliable kinematic system while it deploys.

Deployable bridge structures provide a solution to post-disaster relief efforts. Due to their transportability and ease of installation, they can be in service at the affected locations within a relatively short timeframe [3]. They have been used for temporary lines of communication and have also been used for military applications throughout the world [1,2,3]. This studies deployable bridges as temporary infrastructure and presents a new alternative design for post-disaster relief applications.

Deployable structures have been classified according to their morphology and kinematics by Honor and Levy [19]. This research will focus on a deployable structure that belongs to the pantographs (scissor) structures subcategory. Scissor structures can be deployed by applying a single point force, which is beneficial given the possibility of a lack of resources after an event. Also, these structures have high reliability during deployment and a large volume ratio between their stowed and deployed states [7,10]. While many applications of scissor structures have been proposed, not many have been formalized and constructed due to the design complexity of the system for deployment [10].

## **2-Design Parameters**

The proposed bridge design is aimed at immediate post-disaster relief applications. Therefore, the design parameters selected are based on the review of immediate needs after historical events and previous studies into mobile structures. The US Army has identified specific needs for short-span bridges for post-disaster relief in its Future Force Plan [11,12].

The lightness of the material is beneficial for the transportation and deployability of the system. Another design variable explored is the location of the bridge deck. By varying the depth of the bridge deck, we scour through (at SLE bottom) and half-through (at the midpoint of SLE) bridge configurations as seen in Figure (1) and Figure (2), respectively.



Fig.1.Location of a bridge deck for a through bridge on a rectilinear translational SLE configuration[30]



Fig.2. Location of bridge deck for a half-through bridge on a rectilinear translational SLE configuration with different member lengths. [30]

The bridge is being designed for AASHTO Strength I limit state with a load combination and load factors defined in equation 1.

$$L = y_D(DL + SDL) + y_L(LL) \quad : \text{equation 1}$$

Where,

$$y_D = y_{D-\max} = 1.25 \quad \text{for components and attachments} \quad [20]$$

$$y_L = 1.75 \quad [20]$$

### 3-Design Strategy

The studies give fundamental descriptions regarding three key features of our bridge structure design: Modularity, Deployability, and Materiality.

As we will see later, to the further analysis of each term, there is no doubt that these three terms can be combined efficiently, covering the above requirements of the emergency bridge. The terms Modularity and Deployability are inextricably linked and, in combination with a selection of proper material, can offer a promising solution.[16]

Firstly, the term modularity is described and analyzed since the bridge will consist of a standard-base, pre-fabricated, repeatable modules, which can create different length configurations due to its adding and abstracting ability. Thanks to modularity, flexibility is an easy step, and the bridge can bridge every gap. The interchangeable components can be kept in storage and adapted to the specific site after the disaster immediately.

The second term is deployability. To achieve the desired objective of a compacted form during transportation, the structure will follow the rules of deployability. It will consist of movable elements, which have to be really packed in a folded state for easy transport and durable and large when being

unfolded for assembly and use. The bridge will be both transportable and transformable. It is transportable because of its ability to relocate and transformable because it can change shape.

In general, transformability is needed to make its transportability easier. Deployability concerns the pre-manufacturing of the elements, pre-assembly of the entire structure in a factory, and unfurling or deploying it on site. The last term is materiality. The bridge must be stable, durable, and long-lasting, both materiality and construction like conventional bridges. It has to be lightweight for easy transportation and installation.[16]

In everyday language, the word modularity is used almost as a synonym for the concept of "composed of parts." In broadest terms, modularization is an approach for organizing complex products efficiently by decomposing complex tasks into more superficial portions so they can be managed independently and yet operate together as a whole. [Mikkola, 2003] Hence, modular refers to the ability to assemble a larger system on-orbit from several individual intelligent units. Modularity is based on the idea of interdependence within and independence across modules. [Baldwin and Clark, 2000] Components used in a modular product must have features that enable them to be coupled together to form the complex form. Modular systems are built from highly independent ("loosely coupled") units/components called modules. [Kamrani and Salhieh, 2002] The interactions between them are few and well defined by specific design rules. Through standardization of interfaces, modularization permits components to be produced separately and used interchangeably without compromising system integrity. Interchangeability

and combinations require that the modules have standardized interfaces and interactions.

[Miller, 1998] Based on derivations from the formula above, Gantes [6], Escrig [37], and Maden et al. [38] provided guidelines and compatibility equations for the geometric design of stress-free deployable structures. By varying the member lengths, the location of the pivot joint, and the modes of translation, [14,21] present a review of different scissor structural mechanisms which reliably provide deployment geometries. Additionally, Chikahiro et al. [13] explored the effects of geometric changes in the SLE structure's internal stresses by varying the angle of the diagonals. The study found that when  $\theta_1$  (Figure 3) is less than 30 degrees, the rate of increase of the member stresses is higher than the rate of growth at angles above 30 degrees. Our study seeks to compare the performance of the various SLE deployable system geometries in the context of a particular application, specifically, a bridge structure.

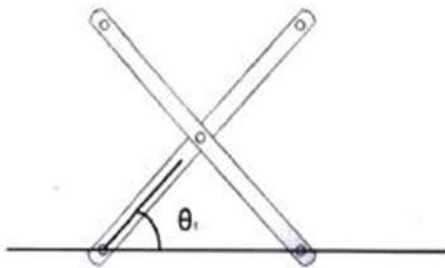


Fig.3. Single SLE unit displaying the location of angle  $\theta_1$  [30]

#### 4-Proposed Concept Design

Following the design parameters outlined of (i) geometry, (ii) weight, (iii) transportability, (iv) performance, and (v) energy required for deployment, we propose a deployable bridge design composed of SLE units. To form a structural system, the units are joined at their external top and bottom nodes to create a lattice. The bridge will be composed of two lattices joined by transversal members supporting the deck.

During the initial exploration phase, small models were constructed to understand SLE-type structures' behavior and ensure that the geometry was feasible for our bridge application. The small-scale models were built at MIT, using wood coffee stirrers for the rigid members and staples for the revolute joints and hinge connections. The lack of vertical and horizontal members, and the fact that the members in each unit are free to rotate at the hinge connections,

allows the system to contract and expand. This characteristic, which facilitates transportability, makes SLE systems a great potential candidate for a deployable structure. An example of a lattice for the SLE bridge model in the deployed and extended condition is shown in Figure (4).

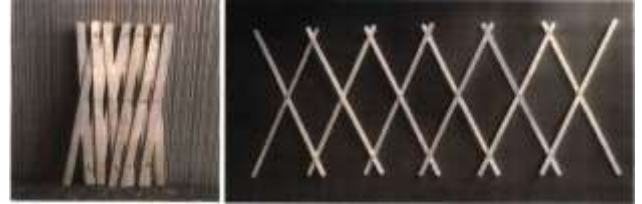


Fig. 4. SLE model or a rectilinear translational geometry made out of wood coffee stirrers and staples. The image on the left shows the structure in its folded position. The image on the right shows the structure in its deployed state at an arbitrary angle. [30]

In this paper, the structure is designed using SLE models but with non-identical dimensions and scattered with different connections in the form of bolts (bean-shaped holes).

#### 5.Scissor Like Element Structures

SLE units are structural units composed of two rigid members. The members are linked together by a common pivot joint, allowing independent rotations along the axis normal to their common plane (Figure 5) [2,6,14].

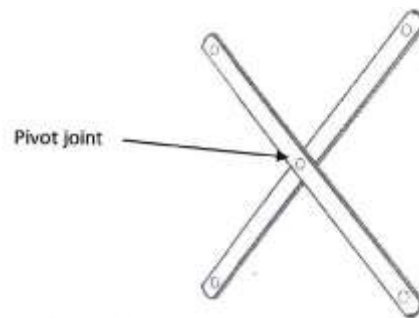


Fig.5. Example of a two dimensional translational SLE unit consisting of two identical rigid beams joined by a single pivot joint in the middle. [30]

Based on the orientation of the unit lines and on the geometry, SLE's are categorized into three basic units: translational (Figure 6 a), polar (Figure 6 b), and angulated (Figure 6 c) [2,22,23]. Translational units have two identical straight members, and their pivot joint is in the middle of the member. When

deployed, the unit lines are parallel to each other. Polar units also have two identical straight members, but the pivot joint offset location creates a curvature during deployment. The unit lines meet at an angle  $\gamma$  which increases during deployment. Lastly, angulated units are characterized by angled

members, which allow the structure to deploy in a radial configuration. The unit lines intersect at an angle  $\gamma$  which remains constant during deployment [2,22,23].

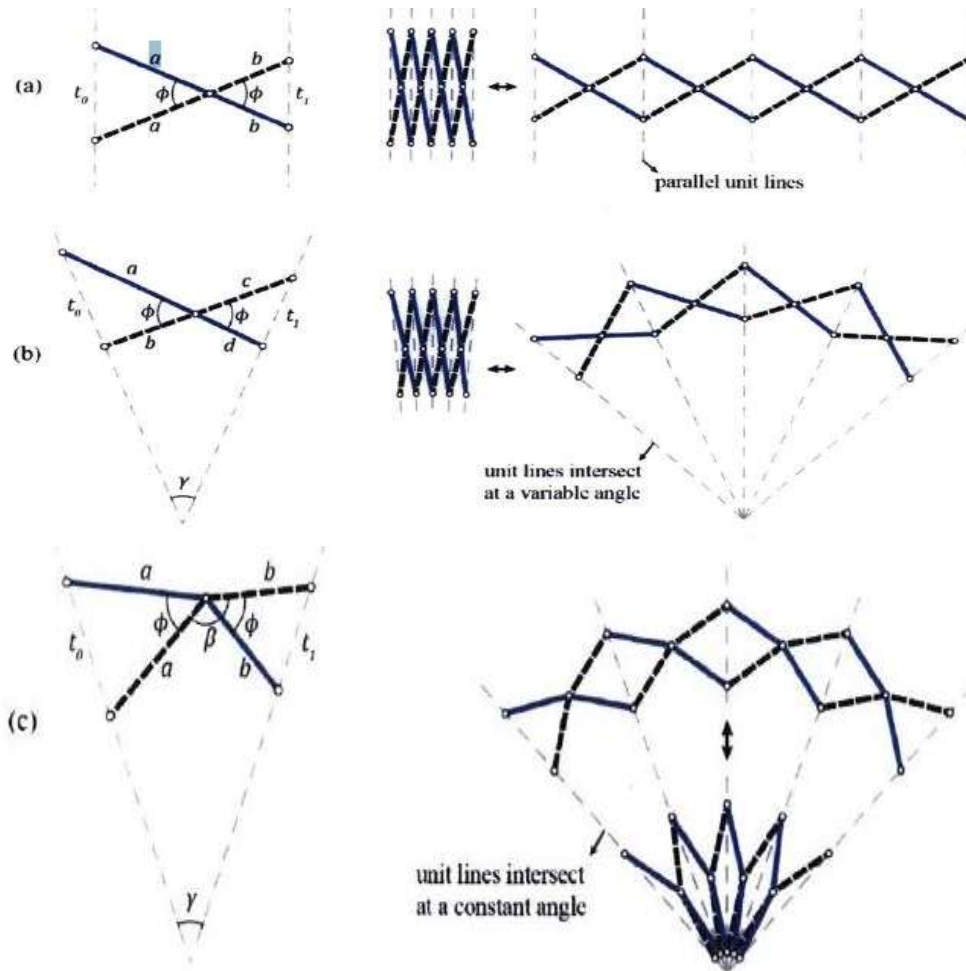


Fig.6. basic unit types in the folded and deployed position: a)translational unit, b)polar unit, c) angulated unit 1381[14]

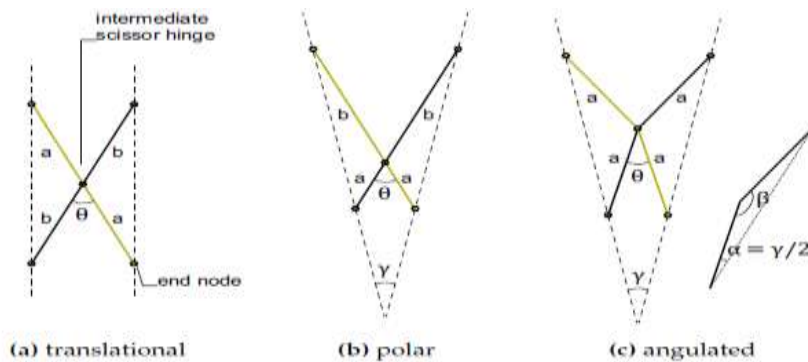


Fig.7. The three traditional scissor types differ in beam shape and intermediate hinge position. The dashed lines are the unit lines. The semi-lengths are indicated by  $a$  and  $b$ ,  $\theta$  is the deployment angle and  $\gamma$  the unit angle. For the angulated type (c),  $\beta$  is the kink angle and  $\alpha$  the angulated angle.[29]

Interconnecting SLE units at their endpoints can form scissor structures. When assembling these structures, geometric considerations must be carefully studied to provide the desired final shape and ensure a compatible and deployable system. Geometric compatibilities define the kinematic behavior and stresses during deployment, depending on the type of SLE unit selected and the overall system geometry. When all the structure members fit together without deformations, i.e., without stresses, it is said that the structure is geometrically compatible. If this compatibility exists at all stages of deployment, then the structure is defined as foldable [24].

Since for a hinge in a scissor unit, only the rotation about the axis perpendicular to the plane formed by the scissor unit must be released,  $C_{rx}$  is equal to zero (Figure 8 b). The other spring stiffnesses are

considered infinitely stiff. However, they are given a high value (1012 kN/m or km/rad) to avoid a poorly conditioned stiffness matrix, leading to inaccurate numerical results in the FE calculations. As a result, in-plane bending is not transferred between beams in a scissor unit, but out-of-plane bending is. In a scissor joint, plural springs come together in one point (Figure 8 c). Since the orientation of the springs' local axes is not straightforward, another approach is required to simulate the scissor kinematics. First, the beam end nodes are stiffly connected to an extra node using zero-length springs, but all stiffness values ( $C_t$  and  $C_r$ ) are very high. By doing so, all beams join in a fixed connection. Afterward, the rotation about the local z-axis is released at the beam end nodes to allow the scissor mechanism (Figure 8 c).[29]

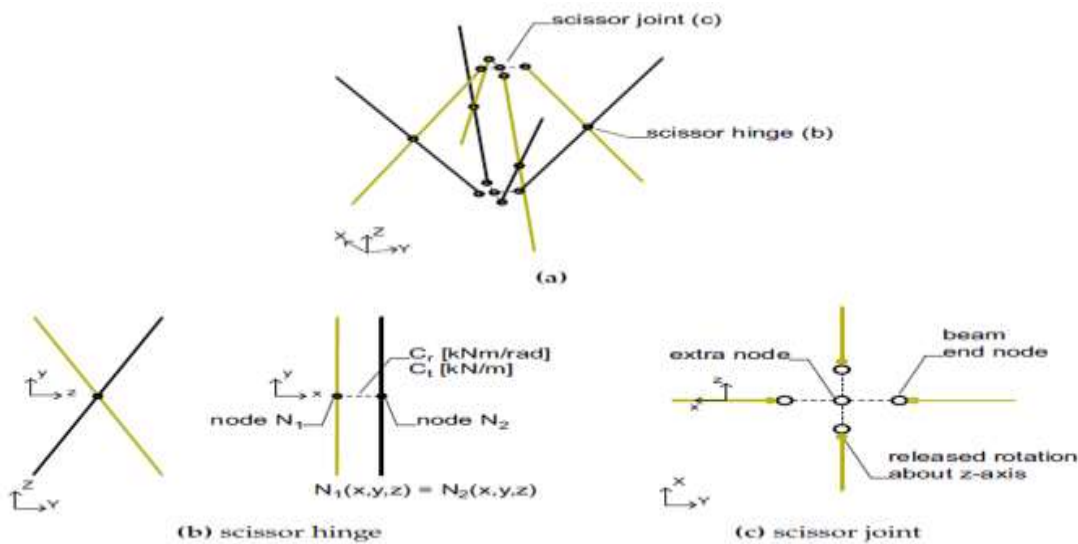


Fig.8.A part of a scissor structure is shown with hinges and joints (a). Scissor hinges (b) and joints (c) are modelled with zero-length springs (dashed lines) with specific rotational  $C_r$  and translational  $C_t$  stiffness properties. XYZ refers to the global and xyz to the local coordinate system.[29]

An essential geometric requirement for a stress-free system is the general deployability condition shown in equation 2. Satisfying equation 2 ensures a stress-free and compatible condition in all members' folded and deployed states. It also provides that when jointed together, SLEs create a system where all members in the linkage reach their most compact state simultaneously. Thus, reducing the link theoretically to a single line, though discrete joint and member sizes dictate the actual size of the system [2,6,24]. However, this condition alone does not ensure geometric compatibility during

deployment [9]. As defined by Gantes and Maden et al., additional considerations need to be satisfied to provide a stress-free deployment and, therefore, a foldable structure [6,14]. These conditions can be met by following derived geometric and trigonometric equations, which relate member lengths, symmetry, deployment angles, total span length, and unit height. These equations and the geometric systems reviewed by Maden et al. [14] are used to develop the deployable bridge design described herein. It should be noted that a foldable structure, although stress-free in the compact and

deployed state, is not stable in the deployed state. Therefore, the system requires the addition of

external locking mechanisms to create a rigid load-bearing structure [6,24].

$$a + b = c + d \quad \text{[equation 2]}$$

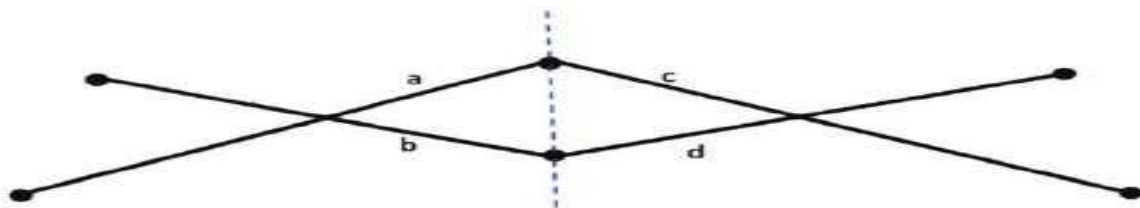


Fig.9 .Geometric constitutive equation required for stress free SLE structures to be stress free in their deployed and folded condition. Reproduced from.[6. 9,21,14]



Fig.10.The different phases during the deployable process.[16]

Hoberman Sphere manifests the designer’s idea of “making structures that transform their size and shape.” The sphere pieces are interlocked and able to spread apart, allowing the structure to contract and expand to a much larger form of its standard size while keeping its shape. Double-armed joints allow scissor-like actions, which maintain the included

angle of the edge throughout the transformation. The Hoberman sphere can be unfolded by allowing certain members to spread apart. The operation of each joint is linked to all the others in a manner conceptually similar to the extension arm on a wall-mounted shaving mirror.[16]

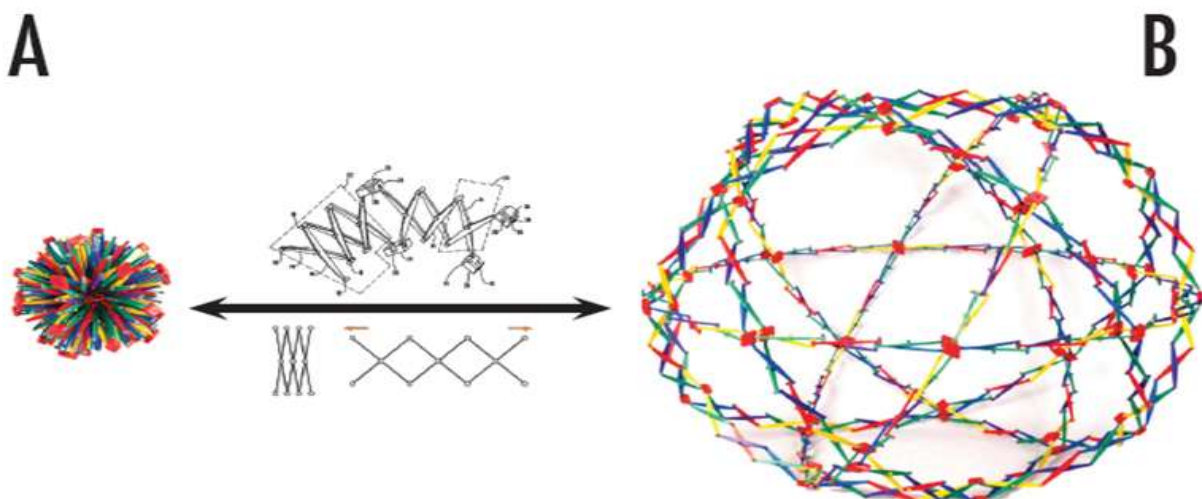


Fig.11. hoberman’s sphere. [16]

Following the calculation of the ultimate rotation capacity of an element, acceptance criteria are defined, labeled IO, LS, and CP in Fig. 6. IO, LS, and CP stand for Immediate Occupancy, Life Safety,

and Collapse Prevention, respectively. This study defines these three points corresponding to 10%, 60%, and 90% use of plastic hinge deformation capacity.

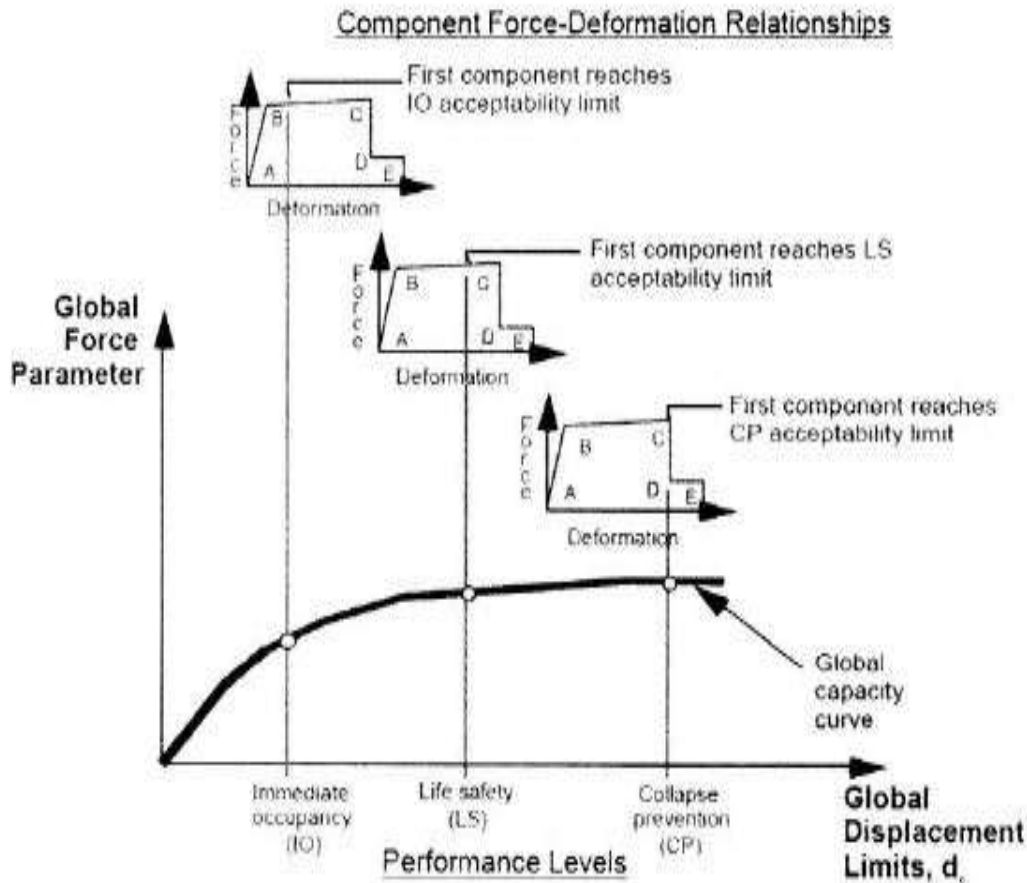


Fig.12.Force–deformation relationship of a typical plastic hinge.(FEMA356)

### 6-General and Physical Characteristics

The bridge in question can be built, installed, and transported in all country regions and has very high efficiency in the area with different climates due to various crises. This bridge connects the two sides of valleys, rivers, canals, and impassable paths and can transport military tools and equipment to the injured

and people. The bridge is made of steel profiles that can be opened and closed; the bridge's total length is 42 meters, and the bridge span is 4.6 meters, which are installed on steel beams. In the main opening of the bridge, all connections are made in the form of bolts and joints and no welding is used.

### 7-Modeling

The bridge is modeled by SAP2000 software, which is based on finite element theory with the capability of nonlinear analysis and overlay. SHELL elements use the cross-section of the steel deck, and the cable

element is used for modeling the cable, which only acts in tension. And a three-dimensional model of the bridge was considered, and the specifications of sections and modeling are given in Table (1).

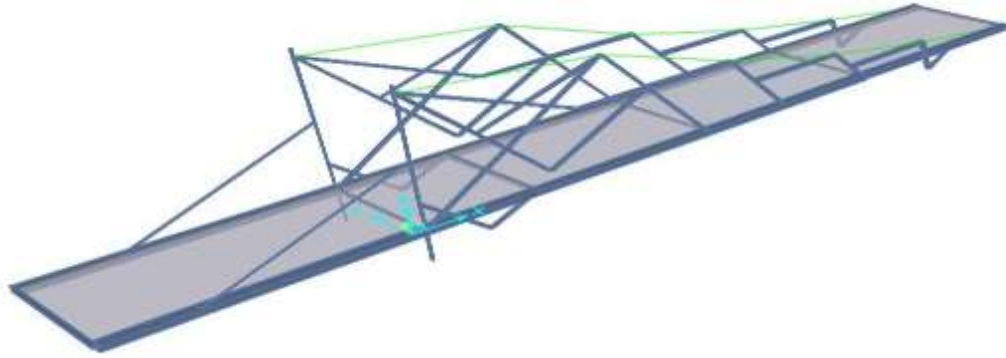


Fig.13. 3D model of the bridge in SAP2000.

Table 1  
Specifications of sections and dimensions of the bridge

Span width	4.6 m
Number of span	1
Bridge length	42 m
Bridge height	12.62 m
Steel Elasticity Coefficient	$2.1 \times 10^6$
Cable section	50 mm
Cable Modulus of elasticity	E=200000 mpa
Number of cables	2
Poisson's ratio	0.3
Shear elasticity coefficient	$0.8 \times 10^6$ Kg/cm
$\gamma$	$7800 \text{ kg/m}^3$

#### 7.1.Mechanical Specifications of Screw Materials

Table (2) presents the mechanical specifications of screw materials in order. [17]

Table 2  
Specifications of Screw Materials

	1	2	3
	Screw category	Fy (kg/cm <sup>2</sup> )	Fu (kg/cm <sup>2</sup> )
1	4.6	2400	4000
2	5.6	3000	5000
3	8.8	6400	8000
4	10.9	9000	1000

#### 7.2.Holes

Table (3) presents the types of holes and their maximum size.

Table 3  
Nominal Dimensions of Screw Holes

(mm) Maximum hole size				Screw diameter (mm)
Long beans (Width) ×(length)	Short beans (Width)×(length)	Large (diameter)	Standard (diameter)	
(d+2)×(2.5d)	(d+2)×(d+7)	d+5	d+2	D

### 7.3.Tighten the Screws

Tightening each screw is done in two steps. First, several screws are tightened to total stiffness to ensure that the contact surfaces are fully bonded, then all screws in the holes are tightened thoroughly. In the second step, the screws are pre-tensioned by turning the nut extra. In each stage of tightening the screws, the screws should be drawn from the part where the connection is tighter and the plates are less deformed. The amount of additional rotation required to prestress the screws is given in Table (4). [17].

Table 4  
Extra Rotation Required to Prestress the Screws[17]

Extra number of turns to prestress the screws	Screw length(L)
1.3 rounds	$L < 4 D$
1.2 rounds	$4 D < L < 8 D$
2.3 rounds	$8 D < L < 12 D$

In this system, an attempt has been made to use all the capacity, and according to Figure (14), it shows how the bridge operates and is installed. Figures (15 and 16) also show the moment distribution of the bridge under live load and the distribution of stresses in the bridge deck. Due to the rapid performance of the structure, the hypothesis has been based on the fact that the bridge can be in different areas due to the embedded elements and its special connections,

### 8-Mechanism of the Bridge

At first, according to the design of the structure and the characteristics of the sections, the primary and secondary beams are entirely made according to the desired dimensions in the workshop. They are connected in a rotating joint, and finally, when they open, they are fixed. Also, steel sections that act as pantographs are installed on top of the beams and to the main pier, opening, closing and retracting.

in all nodes and connections, a constraint has been defined that Rotational constraints should be free in the direction of the bridge length and closed in other directions. The reason for the constraints in the nodes and connections of the structure is because it is possible to show the actual performance of the structure due to its pantograph but with dissimilar components.



Fig.14. Operation of the Bridge

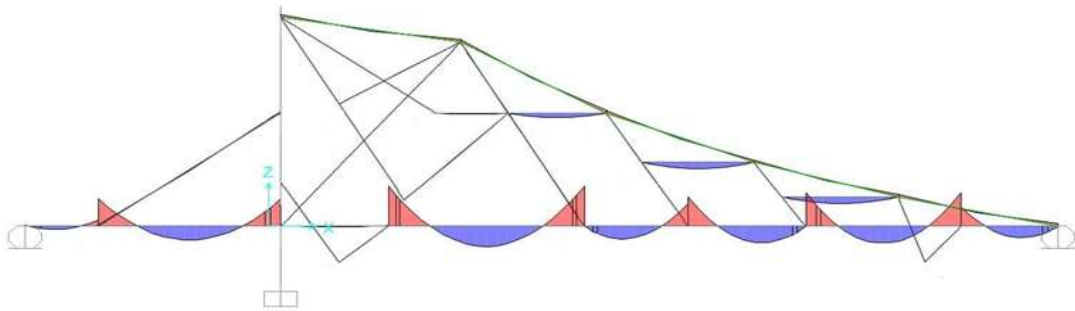


Fig.15. Moment Distribution Diagram of a Bridge under Live Load

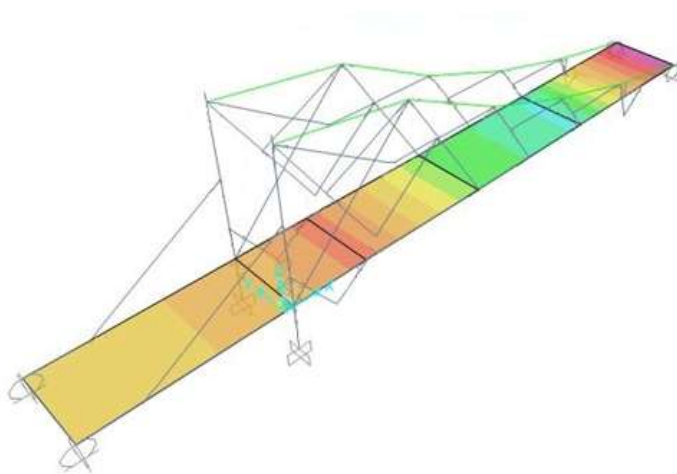


Fig.16. Graphic Representation of Stress Distribution in the Bridge Deck

### 9-Validation

The model studied in the reference [28] has been used to validate the modeling and review the

software results. The data of the cable bridges in question are as follows:

#### 9.1.Geometry of Bridge

Table 5

Geometry of Bridge	
Central Span of the Bridge	253 m
Width of Bridge	12.5 m
Side Span	126.5 m
Height of Pylon	L/4 to L/5 (50m-63m)
No. of Cables	32 nos
Cable Arrangement	Fan type
Girder section	Plate type
Shape of pylon	H , Y type

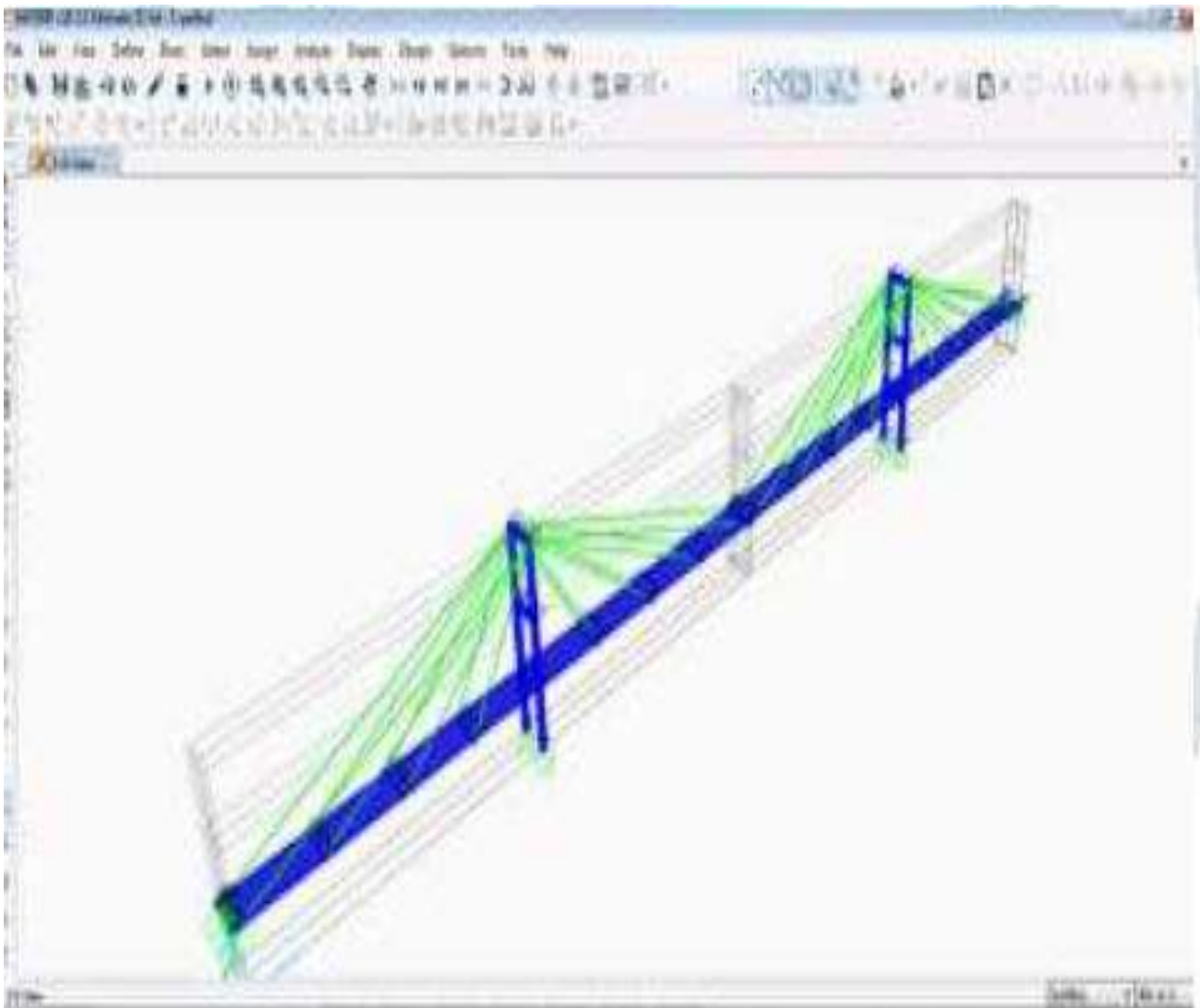


Fig.17. Model of Cable Stayed Bridge[28]

### 9.2. Time Period of 63 m H-shape

Table 6  
Time Periods

Mode	Period(s)	Frequency(syc/sec)	
1	7.6268	0.875	
2	4.1158	1.065	
3	4.1126	1.322	
4	4.1254	1.356	
	5	4.1289	1.426
	6	4.1236	1.458
	7	4.1222	1.723
	8	4.1325	2.323
	9	4.1344	3.122
	10	4.1385	3.256
	11	4.1398	3.984
	12	4.1352	4.252

Table 7  
Pylon Axial force  
**Height of Pylon  
(m)**  
63

**Cable Axial Force(kN)**  
**H-shape**  
59.78

The results of SAP2000 software are presented in Tables (6) and(7). As can be seen, the quantities obtained from cable bridge modeling in the software are close to the results obtained from the reference. [28]

Therefore, this confirms the correct performance of the software and the accuracy of modeling in cable bridge analysis

### 10-Load Patterns

Different load patterns were used to represent the load intensity produced by an earthquake. The first pattern, the Uniform Pattern, is based on lateral forces proportional to the total mass assigned to each node. It can be applied to bridges as:

$$F_i = m_i * g \quad (\text{equation 3})$$

where  $F_i$  = the lateral force at node  $i$  ( $i = 1, 2, \dots, N$ ),  $N$  = number of nodes,  $m_i$  = mass assigned to node  $i$ , and  $g$  is the ground acceleration. FEMA-273 [1] requires using two load patterns (the Uniform Pattern and one of the other two load patterns) and takes the maximum value for each action. This loading pattern emphasizes the base shear rather than giving high moments and deformations.

The second load pattern for bridges, which is called the Modal Pattern in this study, can be written by using load pattern distribution according to the first mode as:

$$F_i = (m_i \phi_i / \sum_{i=1}^N m_i \phi_i) V \quad (\text{equation 4})$$

where  $F_i$  = the lateral force at node  $i$  ( $i = 1, 2, \dots, N$ ),  
 $N$  = number of nodes,  $m_i$  = mass assigned to node  $i$ ,  
 $\varphi$

$\varphi_i$  = amplitude of the fundamental mode at node  $i$ ,  
and  $V$  = base shear.

This pattern may be used if more than 75% of the total mass participates in the fundamental mode of the direction under consideration [1]. The value of  $V$  in the previous equation can be taken as an optional

value since the distribution of forces is important while the values are increased incrementally until reaching the prescribed target displacement or collapse. The third load pattern, which is called the Spectral Pattern in this study, should be used when the higher mode effects are deemed to be important. This load pattern is based on modal forces combined using SSRS or CQC method. It can be written as:

$$F_i = (m_i \delta_i / \sum_{i=1}^N m_i \delta_i) V \quad (\text{equation 5})$$

where  $F_i$ ,  $m_i$ ,  $N$ , and  $V$  are the same as defined for the Modal Pattern (Eq. 2), and  $\delta_i$  is the displacement of node  $i$  resulted from response spectrum analysis of the structure (including a sufficient number of modes to capture 90% of the total mass), assumed to be linearly elastic. The appropriate ground motion spectrum should be used for the response spectrum analysis.

### 10.1. Modal Pushover Analysis Methods with Fixed Load Pattern

To consider the effects of higher modes, various advanced pushover methods have been proposed based on the concepts of structural modal composition. The simplicity of traditional pushover methods is preserved, and the applied load pattern is still assumed to be constant during the analysis. The concepts of modal composition are used in different ways in the proposed pushover methods, which can be divided into two main groups.

(A) In the first group, the rules of combining modes are used to determine the load pattern, and the load pattern is determined by combining load patterns appropriate to the first few ways. Lateral loads based on the determined load pattern are applied incrementally in pushover analysis to the structure. In this method, although the effects of

higher modes are reflected in the applied load pattern, however, the shape of the applied load pattern is limited to a single fixed shape, and the resulting pushover curve (capacity spectrum) is ultimately the same as the capacity spectrum of a system of one degree of freedom. Appears in the form of a fixed hypothetical mode. In fact, the same problems of traditional pushover analysis persist in these methods. Obviously, predicting the response of a system of several degrees of freedom through the response of a system of one degree of freedom can not be done correctly.

B) In the second group, instead of using a push analysis with a combined load pattern, several independent pushes analyzes with load patterns appropriate to each of the desired modes are used. The answers obtained from each mode are combined using modal combination methods. In the popular Modal Pushover Analysis (MPA) method proposed by Chopra and Goel [16], the target displacement is determined independently in each modal pushover analysis, and the responses from each mode are combined. The response of a multi-degree of freedom system is obtained by blending the responses of several systems of one degree of freedom. Because in higher modes, the increase in roof displacement is not commensurate with the changes in displacement of other floors, in some cases, it may even be due to the formation of a mechanism in the structural system for movement, the roof displacement is in the opposite direction and decreases with increasing leg shear. Find. To solve this problem, Hernandomentz et al. [18] have proposed a method of push-modal analysis based on the concept of energy.

### 10.2. Modal Pushover Analysis Methods With Adaptive Load Pattern

In all modal pushover methods described so far, the applied load patterns were constant during the analysis and were determined based on the dynamic elastic characteristics of the structure. Several overlay analyses with adaptive load patterns have been proposed to consider the effects of changes in modal properties in inelastic regions.

In these methods, the applied load pattern in each stage of the analysis is based on the adaptive instantaneous modal characteristics of the structure,

and the changes made in the dynamic characteristics of the structure due to the formation of joints and plastic deformations are considered.

### 10.3. Analysis of an Adaptive Modal Pushover for Seismic Evaluation of Bridges

Considering the fundamental differences between the structural behavior of bridges and buildings and by studying the advanced pushover methods presented in recent years in the case of building structures, a modal pushover analysis method with an adaptive load pattern to evaluate the seismicity of bridges is presented. The proposed method is inspired by the idea used in the Adaptive Modal Combination method (AMC), which combines the Modal pushover Method (MPA) and the Adaptive Modal pushover Method, and has the advantages of both ways. Also, due to the determination of the displacement characteristic in the capacity curve based on the sum of work done on all supports and the use of the concept of energy, ambiguities Existing about the selection of the displacement control point (base support) in the case of bridges has been eliminated. In developing the proposed method, three general concepts have been used, which are:

1) Using the concept of modal analysis and performing several pushover analyses with a load pattern appropriate to each mode.

2) Using the adaptive load pattern in each mode based on the instantaneous modal characteristics of the structure and considering the effects of changes in the instantaneous modal characteristics of the structure due to plastic deformations.

3) Converting the cover curve of the multi-degree-of-freedom system to the system capacity spectrum of one equivalent degree of freedom based on the instantaneous modal characteristics and the total work done on all supports.[e1]

### 11-Push Over Analysis

In this diagram, from which the most important outputs are obtained is the capacity curve of the structures, with the help of which the stiffness and ductility of the structures can be compared. In the nonlinear static analysis method, we design the structure for a target displacement. And shows the strength and deformation in the structure according to the applied earthquakes, which is compared with the capacity of the structure. The amount of ductility, excess strength, energy, and stiffness of the structure can be seen in Figure (18).stiffness of the structure can be seen in Figure (18).

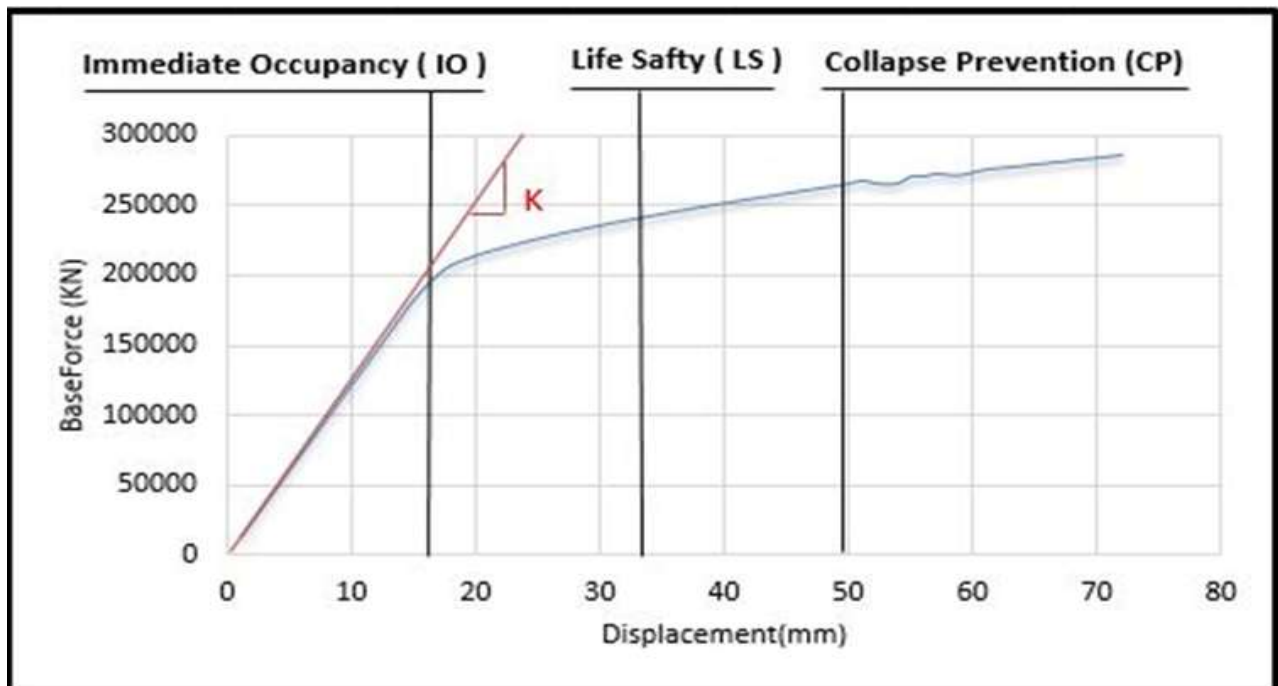


Fig.18. Pushover diagram

Table 8

Target displacements for performance level

Performance Level	IO	LS	CP
FEMA -356	15mm	48mm	53mm

The results obtained from Pushover Analysis shows that the bridge collapses before reaching the

Target Displacement. For FEMA-356, the failure is concentrated and distributed over the length of the bridges.

In Figure (19), the loading is done cyclically (reciprocating) and the element is alternately tensioned and pressured, which consists of several loops, resulting from different loading cycles.

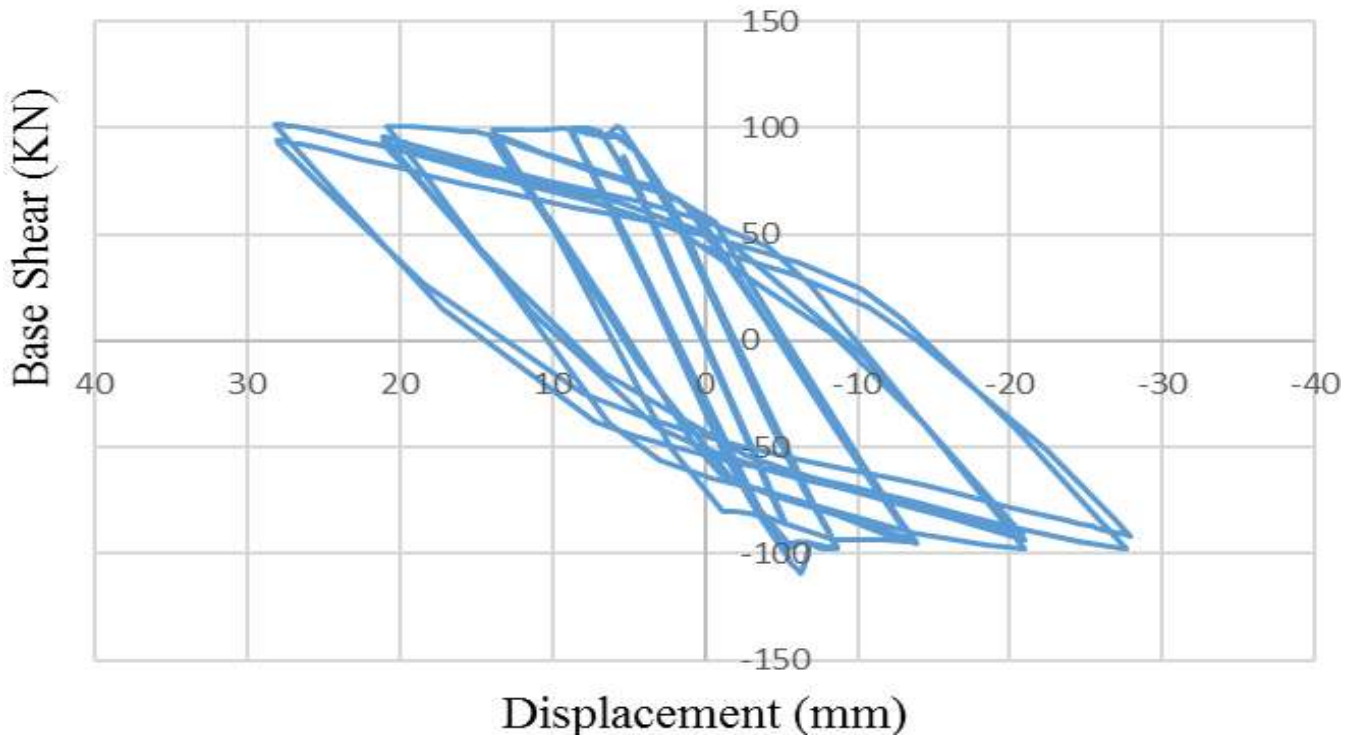


Fig.19. Hysteresis Diagram Related to Connection Number 22 in the Diagonal Member

The number of cycles that an element can withstand before Fracture indicates the reliability and stability of the member, and the higher the symmetry of the curve under tensile and compressive loads, the monotony of the member's behavior under periodic

loads. The area below the chart, or in other words, the area enclosed between the hysteresis charts, indicates the energy consumed by the member. The larger this level, the more ductile the member is and the more power it can absorb.

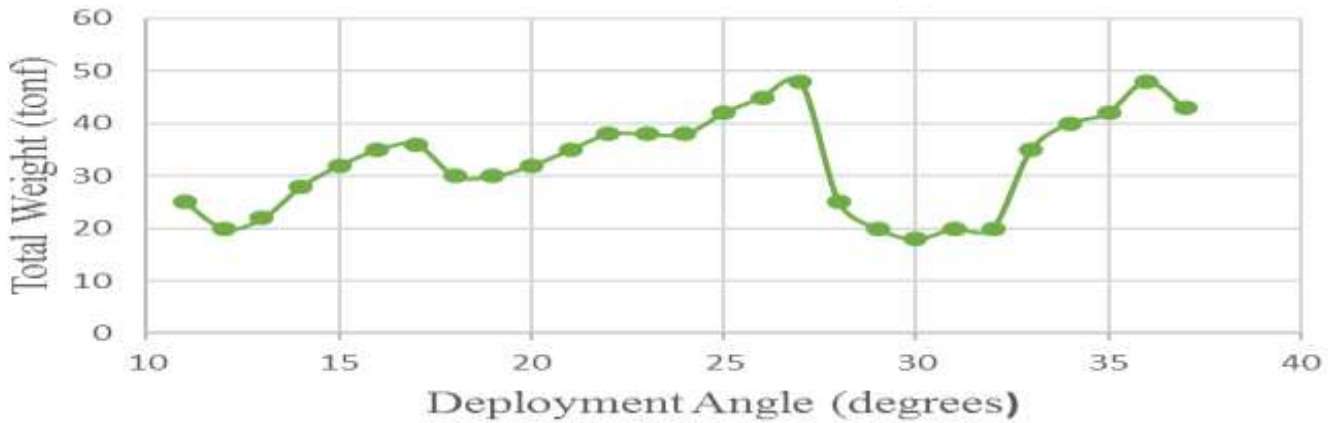


Fig.20 .Minimum weight wolutionsfor all angles

**11.1.Introduction of used Earthquakes**

For nonlinear dynamic analysis of bridges as well as for nonlinear dynamic analysis of the system, one degree of nonlinear freedom to find the target

displacement for incremental analysis used three records, Kobe, Sanfernando, and Superstition .their specifications are given in Table (5).

Table 9  
Records specifications

ID NO.	Earthquake			Station Name	Soil Data NEHRP	Rjb (km)
	Magnitude	Year	Name			
1	6.54	1987	Superstition Hills-02	Superstition-Mtn Camera	C	5.61
2	6.9	1995	Kobe, Japan	Nishi-Akashi	C	7.08
3	6.61	1971	San Fernando	Lake Hughes	C	13.99

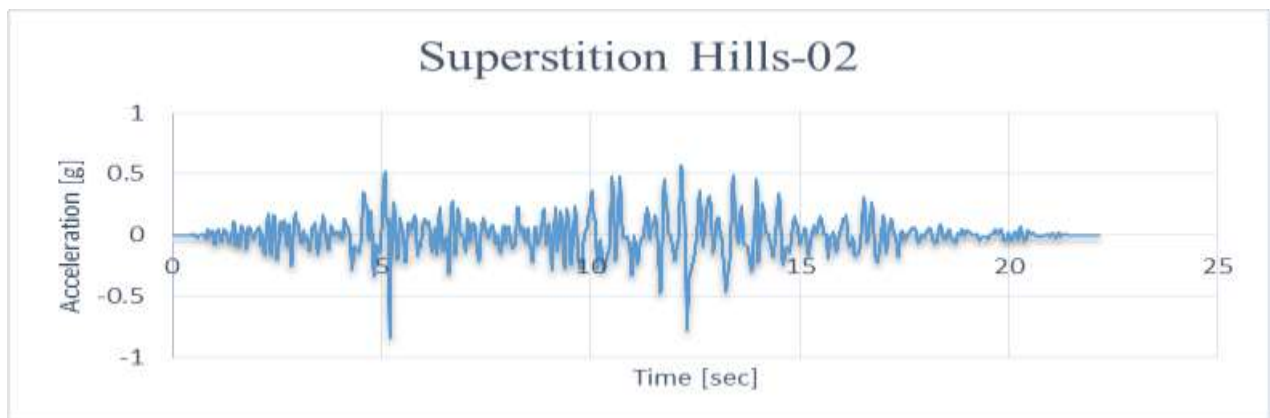


Fig.21. Earthquake Acceleration Applied Superstition to the Structure

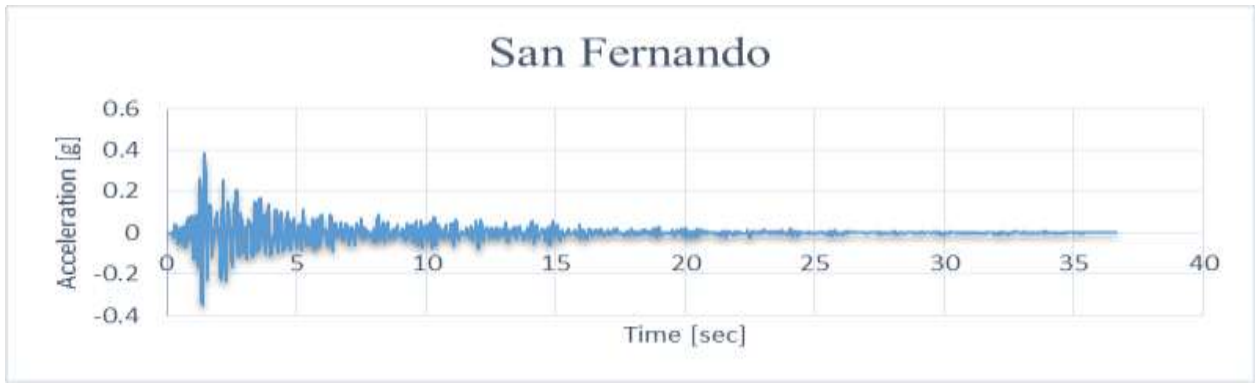


Fig .22. Earthquake Acceleration Applied Sanfernando to the Structure

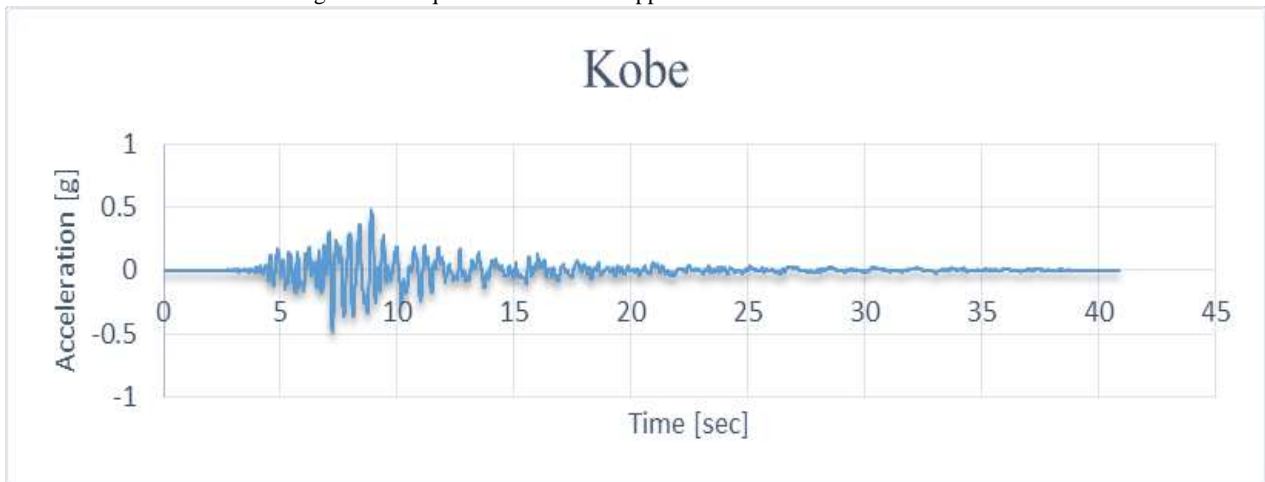


Fig.23. Earthquake Acceleration Applied Kobe to the Structure

Figures No. (21, 22 and 23) show the applied records of the earthquake to the bridge structure and in this

section the lateral displacement of the highest point of the bridge piers is shown.

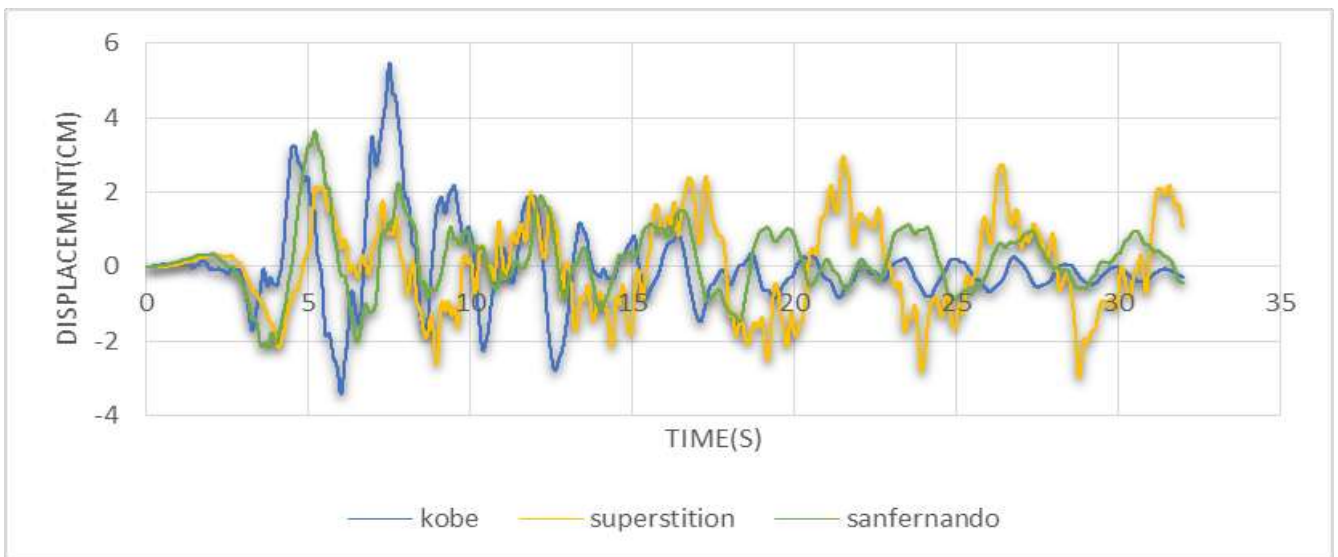


Fig.24. Lateral Displacement of the Highest Point of the Bridge Piers

From the diagrams above, it can be seen that the most displacement occurred in the structure in Kobe earthquake and then in Sanfernando earthquake and the least displacement occurred in Superstition earthquake. The Maximum deck flexural moment due to the applied earthquakes according to Figure

(25) is related to Kobe earthquake and the highest axial force according to Figure (26) is related to Superstition earthquake. And the highest torsional moment according to Figure (27) is related to the Kobe earthquake.



Fig.25. Maximum Deck Flexural Moment Due to Records (KN.m)



Fig.26. Maximum Axial Force of Bridge Piers Due to Records (KN)

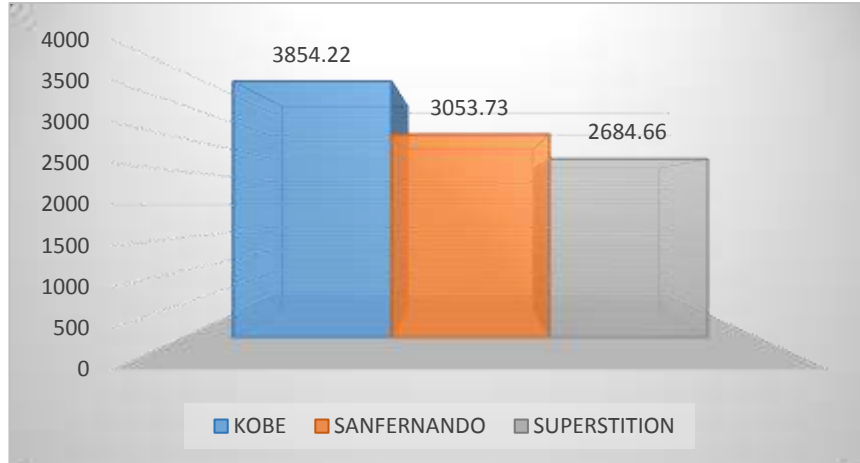


Fig.27. Maximum Torsional Moment Deck Due to Records (KN.m).

## 12- Assessing the Condition and Acceptance Criteria of Structure Joints

Figure (28) shows the process of plastic joint formation in the bridge structure under load distribution. Examining the distribution of plastic

joints, it is observed that the progress of the joints in the bridge is well done and indicates that the maximum capacity of the structure against the incoming loads has been used. Also, the formation of many joints in this structure confirms the correct design.

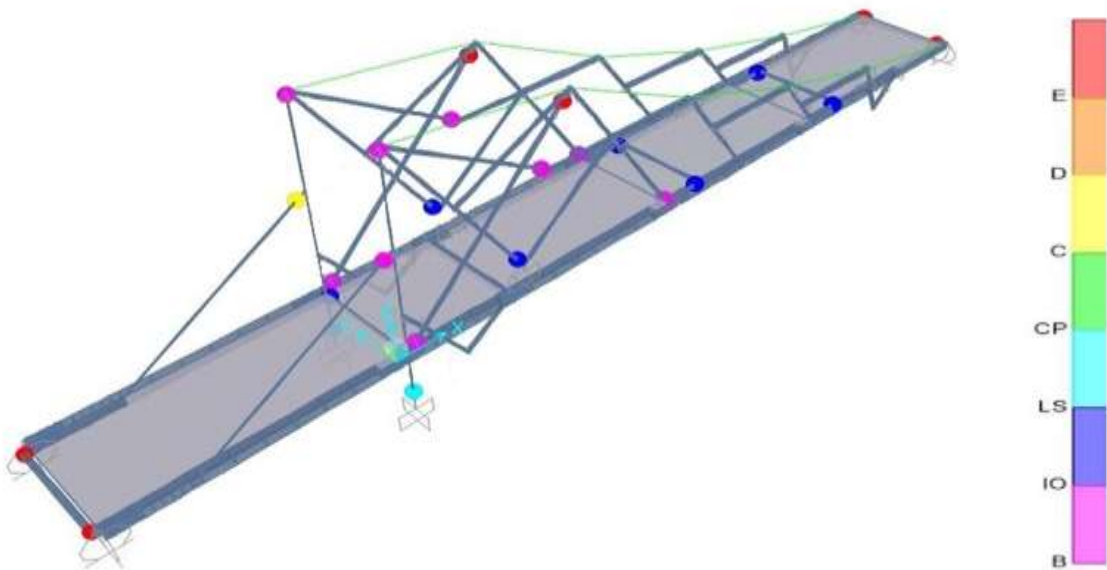


Fig.28. Distribution of Plastic Joint for Bridge

Axial is plastic axial load at hinge, moment is plastic moment at hinge, U1 is plastic axial displacement at hinge, R3 is plastic rotation at hinge, and State is the hinge state at the load between linear and failure load.

Hinge states: A is starting point, B is cracking load, C is yielding load, D is ultimate load and E is failure load. State A to B is linear, B to C is between cracking and yielding, C to D is between yielding and ultimate load, D to E is between ultimate and failure load.

Table 10  
List of joints produced in the software

HINGE	TYPE	Behavior	Generated	From
104H2	Interacting P-M2-M3	Deformation Controlled	YES	Pier
105H1	Interacting P-M2-M3	Deformation Controlled	YES	Pier
105H2	Interacting P-M2-M3	Deformation Controlled	YES	Pier
106H1	Interacting P-M2-M3	Deformation Controlled	YES	Pier
106H2	Interacting P-M2-M3	Deformation Controlled	YES	Pier
107H1	Axial P	Deformation Controlled	YES	Pier
107H2	Axial P	Deformation Controlled	YES	Pier
108H1	V2	Deformation Controlled	YES	Beam
108H2	V2	Deformation Controlled	YES	Beam
109H1	V2	Deformation Controlled	YES	Beam
109H2	V2	Deformation Controlled	YES	Beam
110H1	Moment M3	Deformation Controlled	YES	Beam
110H2	Moment M3	Deformation Controlled	YES	Beam
111H1	Moment M3	Deformation Controlled	YES	Beam
111H2	Moment M3	Deformation Controlled	YES	Beam
112H1	Moment M3	Deformation Controlled	YES	Beam
112H2	Moment M3	Deformation Controlled	YES	Beam

Table 11  
Parameters and Acceptance Criteria for Nonlinear Procedures Beams

Joints	Modeling Parameters			Acceptance Criteria		
	Plastic Rotation Angle,Radians		Residual Strength Ratio	Plastic Rotation Angle, Radians		
	a	b		Primary		
				IO	LS	CP
B-1	90y	110y	0.6	0y	60y	80y
B-2	40y	60y	0.2	0.250y	20y	30y
P-2	0y	1.50y	0.2	0.20y	0.50y	0.80y
P-1	90y	110y	0.6	0y	60y	80y

Table 12  
Frame hinge property data for B-13 (Force\_Displcement)

Point	Force/SF	Disp/SF
-E	-0.8	-17
-D	-0.8	-15
-C	-1.45	-15
-B	-1	0
A	0	0
B	1	0
C	1.45	15
D	0.8	15
E	0.8	17

Table 13  
Frame Hinge Property Data for P-2 (Moment\_Rotation)

Point	Moment/SF	Rotation/SF
-E	-0.6	-11
-D	-0.6	-0.9
-C	-1.27	-9
-B	-1	0
A	0	0
B	1	0
C	1.27	9
D	0.6	9
E	0.6	11

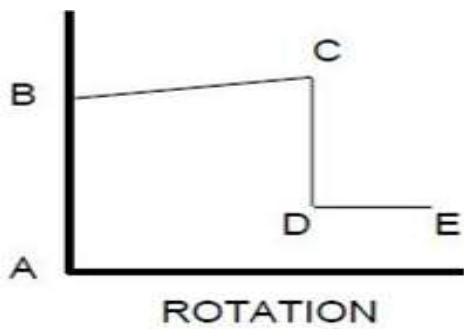


Table 14  
Hinge results for Modal Pushover Plastic (Moment\_Rotation)

HINGE	Axial KN	Moment kN-m	U1 m	R3 Radians	State
H1	0	258.36	0	0	A to B
H2	0	-243.63	2.5E-08	-6.44E-05	A to B
H3	0	-589.23	0	0	A to B
H4	0	-725398	0	0	A to B
H5	0	-635.25	0	0	A to B
H6	0	-578.32	2.56E-4	-5.33E-04	A to B
H7	0	-452.36	0	0	A to B
H8	0	-335.12	0	0	A to B
H9	0	-225.236	0	0	A to B
H10	0	-152.36	0	0	A to B
H11	0	452.688	0	0	A to B

Table 15

Frame hinge property data for P-2 (Moment\_Rotation)  
Hinge results for Modal Pushover Plastic (Axial\_Moment\_Rotation)

HINGE	Axial	Moment	U1	R3	State
	KN	kN-m	m	Radians	
H1	2932	24.12	0	0	B to C
H2	2932	-33.25	4.5E-06	-5.46E-05	B to C
H3	2932	-45.75	3.6E-08	0	C to D
H4	2932	-55.23	0	0	B to C
H5	2932	-65.25	2.8E-08	0	A to B
H6	2932	-68.15	2.566E-4	-6.85E-04	A to B
H7	2932	-75.23	0	0	B to C
H8	2932	-55.32	4.5E-08	0	C to D
H9	2932	-32.45	0	-5.5E-08	A to B
H10	2932	-142.56	4.78E-08	0	B to C
H11	2932	26.96	0	0	B to C

### 13-Conclusion

This paper tries to propose a structural design for an installed bridge structure. We find that the best geometry concerning the objective function consists of several units of asymmetric sections that are applied along their unit line with different half-deck positions and angles. In addition, the rigid rods that make up the SLE unit have different lengths while our bridge can be extended.

This study presents a system that is a competitive solution for the proposed program based on the performance of the minimum weight target. Due to the possible lack of resources after a natural disaster, providing a lightweight, easily portable, and scalable structure that requires less workforce and resources for installation can positively impact the recovery process. Possibility of assembling and dismantling the structure in each stage of execution and after execution, ease of packing and loading and transporting the structure to all points, low weight of structural elements, structural safety, load sharing capability, high stiffness, stress distribution in all directions safety factor The top of the structure

against storms, earthquakes and fires are among the advantages of this system.

The distribution of plastic joints shows ductility, durability, and strength in the bridge structure. It also indicates that the total capacity of the structure against earthquakes has been used.

### References

- [1] [1] M. Saatcioglu, A. Ghobarah, I. Nistor. (2006), Performance of Structures in Indonesia during the December 2004 Great Sumatra Earthquake and Indian Ocean Tsunami, Earthquake Spectra, vol. 22, no.3, 2006, pp. 295-319.
- [2] J.C. de la Llera, F. Rivera, J. Mitrani-Reiser, R. Junemann, C. Fortuno, M. Rios, M.Hube 1, H. Santa Maria, R. Cienfuegos. (2017), Data Collection After the 2010 Maule Earthquake in Chile, Bull Earthquake Eng. vol.15, pp. 555 - 588.
- [3] B.R. Russell, A.P. Thrall. (2013), Portable and Rapidly Deployable Bridges: Historical

- Perspective and Recent Technology Developments, Journal of Bridge Engineering, vol. 18, no.10, pp. 1074 -1085
- [4] Y.Wang, A.P. Thrall, T.P. Zoli. (2016), Adjustable Module for Variable Depth Steel Arch Bridges, Journal Constructional Steel Research, vol. 126, pp. 163-173.
- [1] C.H. Hernandez Merchan, (1987), Deployable Structures, Master's Thesis Department of Architecture, Massachusetts Institute of Technology, Cambridge, Massachusetts.
- [2] C.J. Gantes. (2001), Deployable Structures: Analysis and Design, WIT Press.
- [3] L. Alegria Mira, N. De Temmerman, C. Preisinger. (2012) Structural Optimisation of Deployable Scissor Structures Using New Computational Methods., WIT transactions on the built environment, vol. 124, pp. 469-480.
- [4] L. Alegria Mira, R. F. Coelho, A.P. Thrall, N. De Temmerman, (2015), Parametric Evaluation of Deployable Scissor Arches, Engineering Structures, vol. 99, pp. 479-491.
- [5] S. Pellegrino. (2001), Deployable Structures, Springer-Verlag Wien New York.
- [6] N. De Temmerman. (2007), Design and Analysis of Deployable Bar Structures for Mobile Architectural Applications, PhD dissertation, Department of Architectural Engineering Sciences, Vrije Universiteit Brussel, Brussels, Belgium.
- [7] G.Lederman,Z.You, Branko Glisic. (20014), A Novel Deployable Tied Arch Bridge, Engineering Structures, vol.70, pp. 1-10.
- [8] M. J. Robinson, P.E.1, J. B. Kosmatka, P.E. (2008), Development of a Short-Span Fiber-
- [9] Reinforced Composite Bridge for Emergency Response and Military Applications,Journal of Bridge Engineering, vol.13, no.4, pp. 388-397.
- [10] Y.Chikahiro, I. Ario, M. Nakazawa. (2016), Theory and Design Study of a Full-Scale Scissors-Type Bridge,Journal of Bridge Engineering, vol. 21, no.9.
- [11] F.Maden,K. Korkmaz, Y. Akgtn. (2011), A Review of Planar Scissor Structural Mechanisms:Geometric Principles and Design Methods, Architectural Science Review, vol. 54, no. 3 , pp. 246 -257.
- [12] K. Roovers, N. De Temmerman. (2017), Deployable Scissor Grids Consisting of Translational Units, International Journal of Solids and Structures, vol. 121, pp. 45-61.
- [13] Elia Galiouna. (2015), An Instant Connection,[designing an emergency, deployable bridge]. Master Architecture, Urbanism And Buildingv Sciences Faculty Of Architecture Delft University Of Technology January.
- [14] AASHTO- standard specification for highway bridges- 16th ed 1996- section 10.
- [15] <http://www.youtube.com/foldingbridge>.
- [16] A. Hanaor, R. Levy. (2001), Evaluations of Deployable Structures for Space Enclosures,International Journal of Space Structures, vol. 16, no. 4, pp. 211-229.
- [17] AASHTO. (2014), Load and Resistance Factor Design (LRFD) Bridge Design Specifications: Customary U.S. units, 7th Ed., Washington, DC.
- [18] F. Escrig. (1985), Expandable Space Structures. Journal of Space Structures.,vol 1, no.2,pp.7991.
- [19] L, Alegria Mira, A.P. Thrall, N. De Temmerman. (2015), The Universal Scissor Component: Optimization of a Reconfigurable Component for Deployable Scissor Structures. Engineering Optimization, pp. 1-17.
- [20] K. Roovers, N. De Temmerman. (2015), Digital Design of Deployable Scissor Grids Based on Circle Packing, Proceedings of the International Association for Shell and Spatial Structures (IASS) Symposium, Amsterdam.
- [21] K. Roovers, N. De Temmerman. (2017), Deployable Scissor Grids Consisting of Translational Units, International Journal of Solids and Structures, vol. 121, pp. 45-61.
- [22] Mikkola, J. H. (2003), Product Architecture Modularity Strategies: Toward A General Theory. Denmark: Copenhagen Business School.
- [23] Baldwin, C.Y. and Clark K.B. (2000), Design Rules.Volum1: The Power of Modularity. London: The MIT Press.
- [24] Kamrani, A. and Salhie, S. (2002), Product Design for Modularity. USA: Kluwer Academic Publishers.
- [25] K. Mavani, A. Raturi, M. Kakadiya.(2018), Parametric Study Of Cable Stayed Bridge For Different Pylon Configuration, JETIR May 2018, Volume 5, Issue 5.